Finite Element Investigation on Load Carrying Capacity of Corroded RC Beam Based on Bond-Slip

Yang Xiaoming* and Zhu Hongqiang

* Corresponding Author. Email: xiao_m_y@163.com
College of Civil Engineering and Architecture, Liaoning Technical University, 47, Zhonghua Street, Fuxin Liaoning 123000, China

ABSTRACT

The finite element (FE) investigation on the load carrying capacity of corroded RC beam is carried out based on the bond-slip between the steel bars and concrete. In the numerical simulation, several FE models of RC simply supported beam with different corrosion ratios were built using ANSYS. In these FE models, element of Solid65 was used to simulate concrete, element of Link8 was used for bars and element of Combin39 was adopted to simulate the bond and bond-slip between bars and concrete. The effect of corrosion ratio on bonding force between bars and concrete was simulated by adjusting the parameter of Combin39. Besides, the reduction of bars section area and decrease of bars yielding stress were also considered for calculating the load carrying capacity of corroded RC beam with different corrosion ratios. The results show that as the corrosion ratio increases the stiffness of corroded beam would decrease, slip between bars and concrete would be larger and ductile failure of RC beam would turn to brittle failure. The load carrying capacity of corroded RC beam would obviously deteriorate and descending speed is the fastest when the corrosion rate falls in the range of 4%-7%.

KEYWORDS: Corrosion, Deterioration of bonding, Load carrying capacity, Numerical simulation.

INTRODUCTION

RC structures are nowadays widely used in civil engineering. However, problems, on durability such as reinforcement corrosion, concrete carbonization, chloride ion penetration, freezing and thawing cycles and alkali-aggregate reaction, make RC structures hard to stay healthy (serviceable) during their service lives. Among these problems, reinforcement corrosion plays a key role and directly threatens the safety and durability of concrete structures (Shi and Sun, 2010; Shodj et al., 2010). How to evaluate these corroded structures and predict their residual capacity is an urgent problem in current civil engineering (Haskett et al., 2008; Coronelli and Gambarova, 2004).

Research methods on load carrying capacity of corroded reinforced concrete components include theoretical analysis, experimental study and numerical simulation. Some new theoretical analysis methods have been recently proposed. Weiliang et al. (2009) proposed the differential equation for the axial force of the longitudinal bar considering deterioration of the rebar, concrete and bonding between the rebar and concrete. Tapan and Aboutaha (2011) developed moment-axial load (M-P) interaction diagrams using modified analysis procedure and advanced deteriorated material models for quantifying the effect of reinforcement corrosion and loss of concrete cover on structural behavior of

Accepted for Publication on 17/10/2011.

bridge columns. Other methods are experimental studies which focused on the selection of corroded sample including electrochemical rapid corroded components, removed practical engineering members, long-term exposed natural components… and so on (Wang et al., 2011; Sharifi and Pei, 2011; Malumbela et al., 2010).

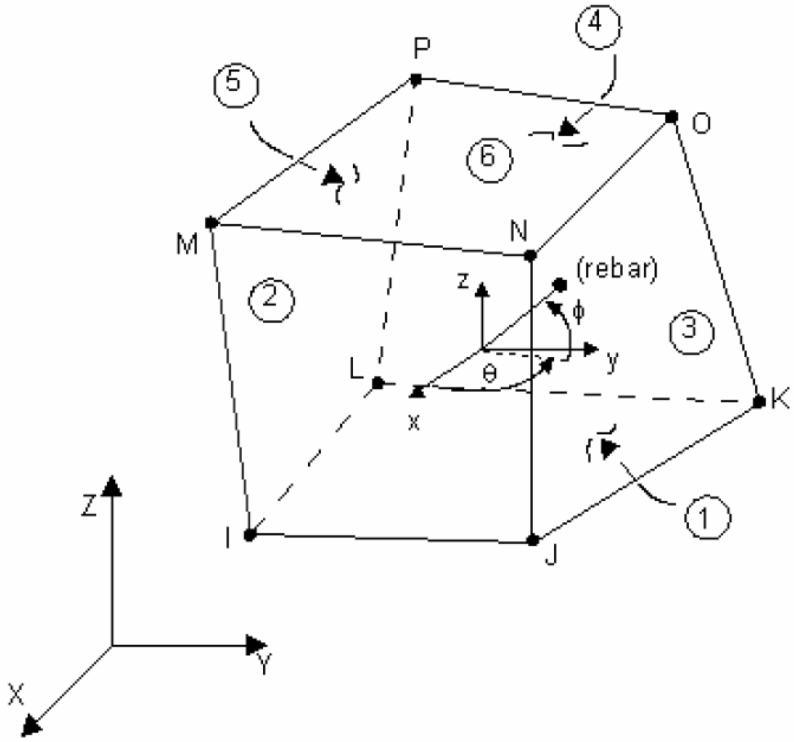

Figure 1: Solid65 element in ANSYS

Numerical simulation is one of the effective methods to analyze the load carrying capacity of corroded reinforced concrete components (Yuan and Ji, 2009). As long as the size of discrete element is suitable and the constitutive relation is correct, the simulation results will reach the real value and satisfy the engineering requirements. Numerical simulation can overcome the disadvantages such as the difference between the rapid corroded components and the practical engineering members, long duration of long-term exposed natural experiments… and so on (Alexandros and Imran, 2010; Bertoa et al., 2008). Besides, numerical simulation without the limitations of experimental conditions and testing technology lets obtain stress of corroded bar, stress distribution in concrete, bond stress and slip values at the bar-concrete interface.

This paper analyses the load carrying capacity of corroded RC simply supported beams using the FE method. In the FE model, Solid65 element in ANSYS was used to simulate the concrete and Link8 element was used to simulate the bar. Because the corrosion of the bar causes the increase of slip at the bar-concrete interface, the physical model of the bonding element and the constitutive relation of vertical and radial bond-slip of corroded bars have a direct effect on the reliability of analysis results of numerical simulation. Combin39 element in ANSYS was adopted to simulate the slip at the bar-concrete interface, and the effect of corrosion ratio on bonding force between bars and concrete were simulated by adjusting the parameter of Combin39 element. Through setting different corrosion rates, the change of component capacity and failure mode were analyzed using the FE models.

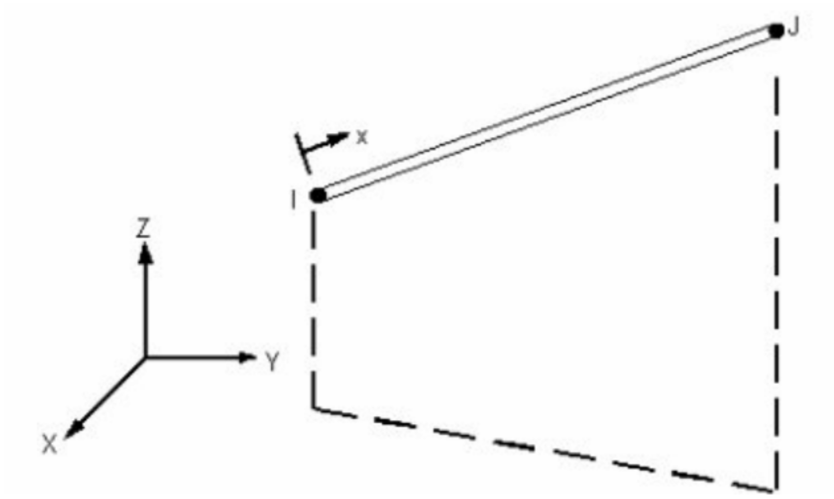

Figure 2: Link8 element in ANSYS

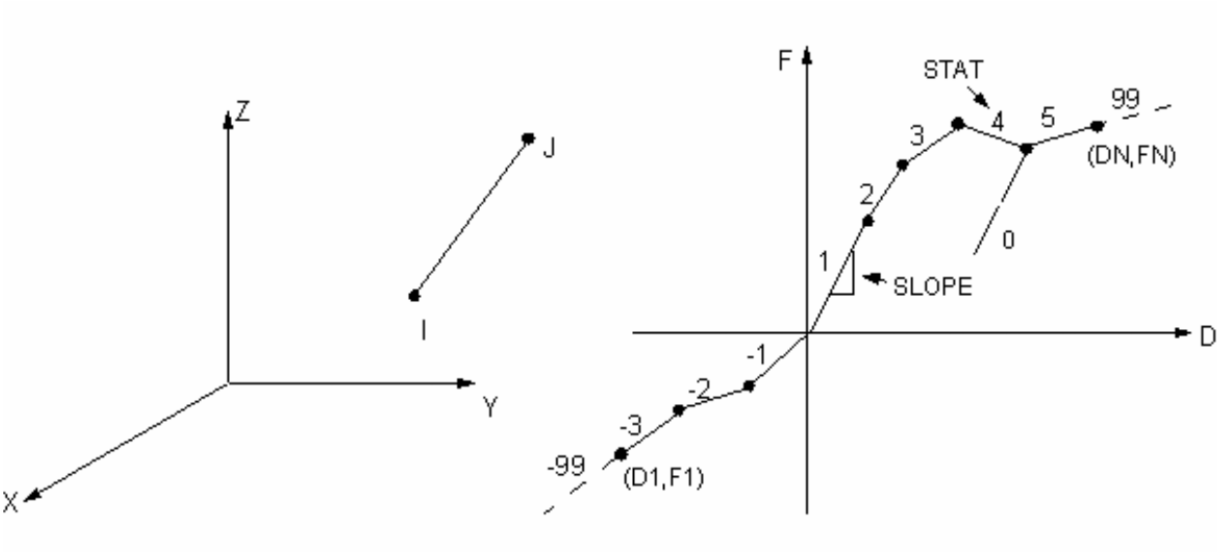

Figure 3: Combin39 element in ANSYS

Finite Element Model

Element for Concrete

Solid65 element with 8 nodes and 3 degrees of freedom (X, Y, Z) in ANSYS, as shown in Fig.1, was used to simulate the concrete, and its nonlinearity was defined by the material attribute table. In this FE model, multi-linear isotropic hardening model under Mises yield criterion was adopted, crack opening shear transfer coefficient and crack closing shear transfer coefficient were defined and the improved William-Warnke5 failure criterion was applied. Five coefficients were input to determine its failure surface (uniaxial tensile strength, uniaxial compressive strength, biaxial compressive strength, uniaxial compressive strength and biaxial compressive strength under a certain confining pressure). Due to the lack of multiaxial experimental parameters, only uniaxial tensile strength and uniaxial compressive strength were input and other parameters were defaulted by ANSYS. Besides, the uniaxial compressive strength was defined as a negative value so as to be convenient to converge, which indicates that the compressive failure surface is invalid and only the tensile softened effect is considered.

Element for Bar

The reinforcing bar was simulated by Link8 element with 2 nodes and 3 degrees of freedom (X, Y, Z), as shown in Fig. 2. It can bear uniaxial tension and compression and can be used to simulate plasticity and large deformation. When corrosion rate is η, the yield strength f_{yc} of the corroded reinforcement needed by the adopted bilinear isotropic hardening (BISO) model can be defined as follows:

$$f_{yc} = \frac{1-1.077\eta}{1-\eta} f_{y0} ; \tag{1}$$

where f_{y0} is the yield strength of the intact reinforcement (300MPa) and η is the mass loss percentage (%) of the corroded bar.

Element for Bonding

In order to exactly simulate the corroded member's mechanical properties, a three-dimensional nonlinear spring element (Combin39, as shown in Fig. 3) was adopted as the bonding element at the bar-concrete interface for simulating its bond-slip relationship. Combin39 element is a nonlinear spring element whose nonlinearity can be defined by inputting the load-displacement relationship. In the separate type of RC model, 3 nonlinear spring elements were established between the relative bar element node and concrete element node along the transverse and longitudinal direction.

The relationship between local bond stress $\tau(s)$ and slip at the non-corroded bar-concrete interface along the longitudinal direction is defined as follows:

$$\tau(s) = \left(61.5.\,s - 693.s^2 + 3.14\times10^3.s^3 - 0.478\times10^4.s^4\right).f_{t,s}.\sqrt{c/d} \tag{2}$$

where *s* is the slip value (mm), *c* is the thickness of the cover layer (mm), *d* is the diameter of reinforcement (mm) and $f_{t,s}$ is the concrete's splitting tensile strength (N/mm^2).

In the FE model of the RC beam, the relationship between the bond force *F* and slip value *s* can be calculated as follows:

$$F(s) = \tau(s).\pi\, dl ; \tag{3}$$

where *d* is the diameter of a bar (mm) and *l* is the distance between two adjacent spring elements (mm).

From Eq.(2) and Eq. (3), the load-displacement relationship (*F-D*) of the spring element along the longitudinal direction can be obtained (see Fig.4).

When the corrosion rate is η, the reduction factor β of the bond strength at the corroded bar-concrete interface can be calculated as follows (Xu, 2003):

$$\beta = \begin{cases} 1 + 0.5625\eta - 0.3357\eta^2 + 0.055625\eta^3 - 0.003\eta^4 & \eta \le 7\% \\ 2.0786\eta^{-1.0369} & \eta > 7\% \end{cases} \tag{4}$$

Substituting Eq.(4) into Eq.(3), the relationship between the bond force *F* and slip value *s* after corrosion can be obtained:

$$F(s) = \beta.\tau(s).\pi\, dl . \tag{5}$$

Thus, the *F-D* curves of the spring element along the longitudinal direction under the different corrosion rates are shown in Fig.5.

Stiffness coefficient K_v of the spring element along the transverse direction can be calculated as follows:

$$K_v = \frac{EB_n l}{b} ; \tag{6}$$

where *E* is the elastic modulus of concrete, B_n is the net width of the beam at the reinforcement position and b is the width of the beam.

The load-displacement relationship (F-D) of the spring element along the transverse direction can be calculated as follows:

$$F = \int_0^D K_V ds = K_V . D . \quad (7)$$

From Eq.(5) and Eq. (7), it can be seen that the load-displacement relationship along the transverse direction is linear, while the load-displacement relationship along the longitudinal direction is nonlinear.

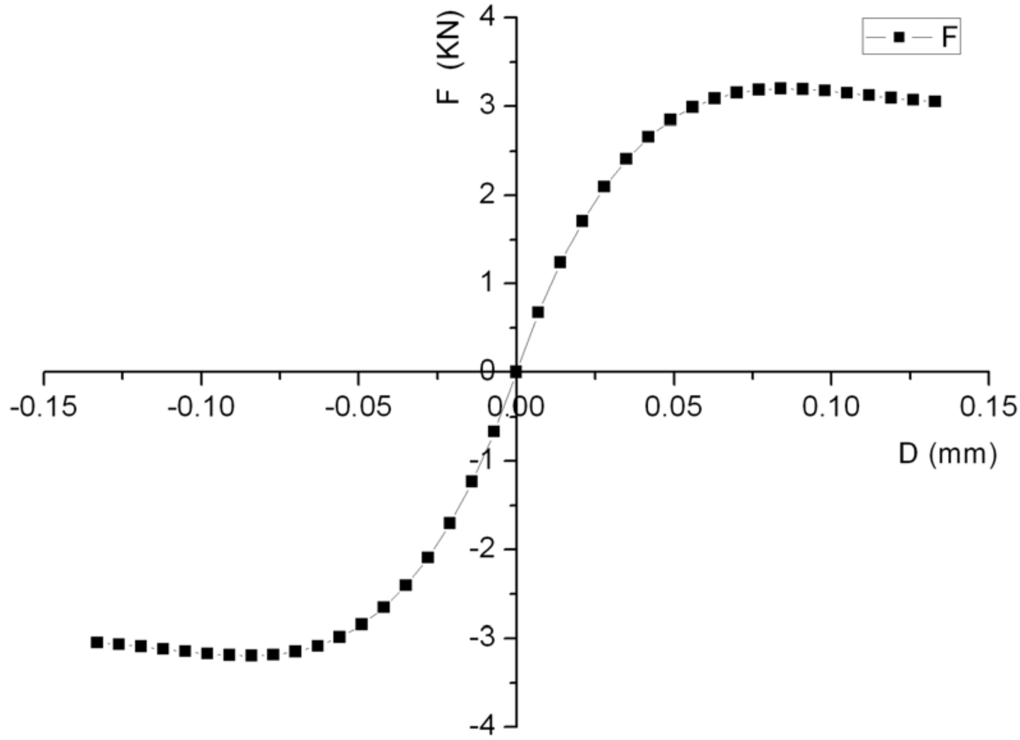

Figure 4: The load-displacement relationship of the spring element along the longitudinal direction

Case Study

The FE model of a simply supported RC beam was selected as an example for analyzing the load carrying capacity of corroded RC beam. The beam's span is 500 mm and the dimensions of its cross-section are 100mm×150mm. In the beam model, top bars are 2Φ4, bottom bars are 2Φ8 and stirrups are Φ4@35mm. The concentrated load is applied in both sides of the mid-span and the distance from the mid-span is 50mm.

The case study includes three steps. First, the nodes of bar element and concrete element node at the same location were consolidated in the FE model, which ignored the slip at the bar-concrete interface. By comparing the simulated load carrying capacity with the theoretical capacity, the validity of the model can be proved. Secondly, Combin39 element was installed between the bar element node of longitudinal bar and the concrete element node to consider the effect of bonding slip at the bar-concrete interface. By comparing its simulated capacity with the results of the first step, the feasibility of the Combin39 element can be verified. Finally, the Combin39 element was modified to consider the influence of the bond deterioration at the bar-concrete interface due to corrosion. Besides, the reduction of bar cross-section area and decrease of reinforcement yield strength were taken into consideration for calculating the load carrying capacity of the simply supported RC beams with different corrosion rates. Thus, the effect of steel corrosion on load carrying capacity of RC beam was analyzed utilizing the model.

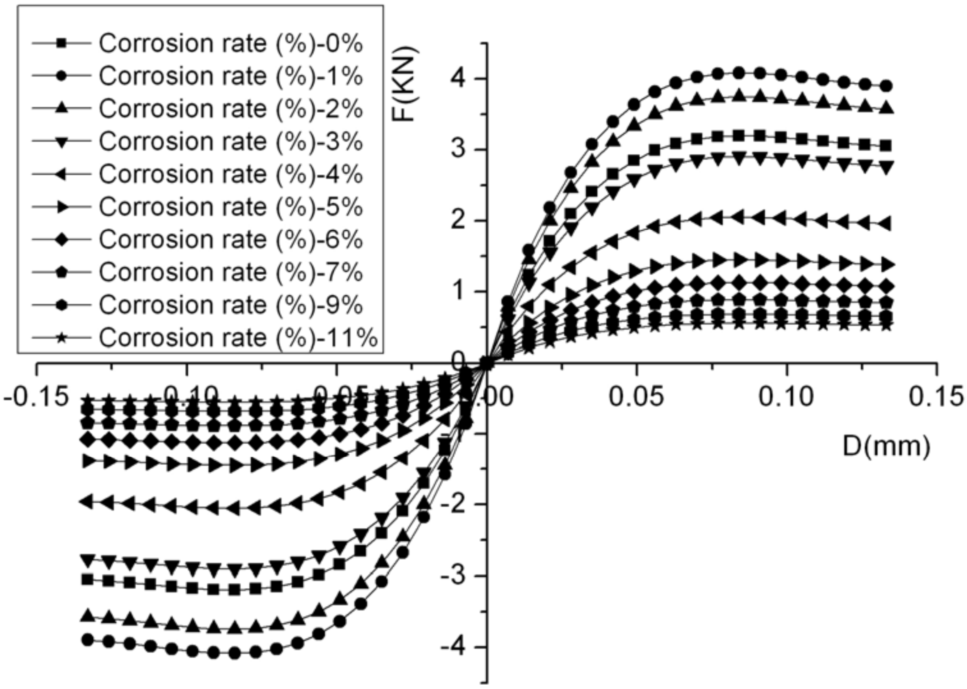

Figure 5: The load-displacement relationship curves of the spring element along the longitudinal direction under different corrosion rates

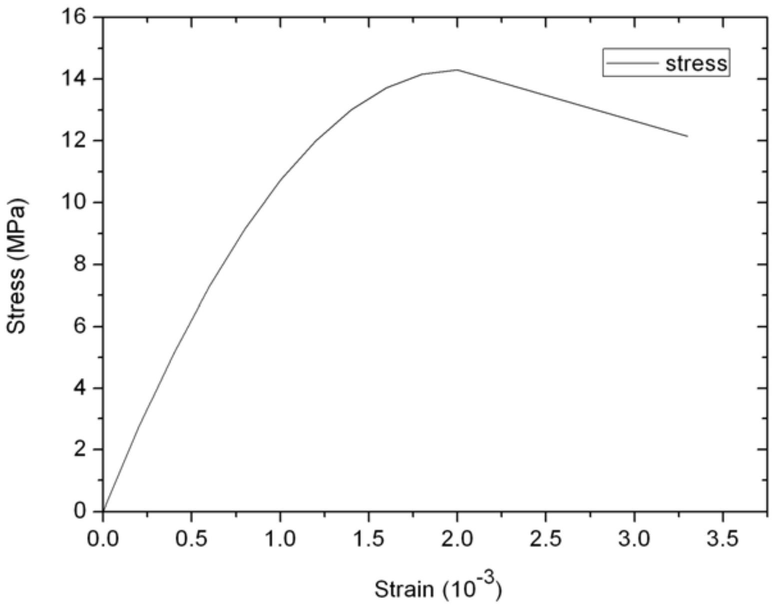

Figure 6: Multilinear isotropic hardening curve of the concrete

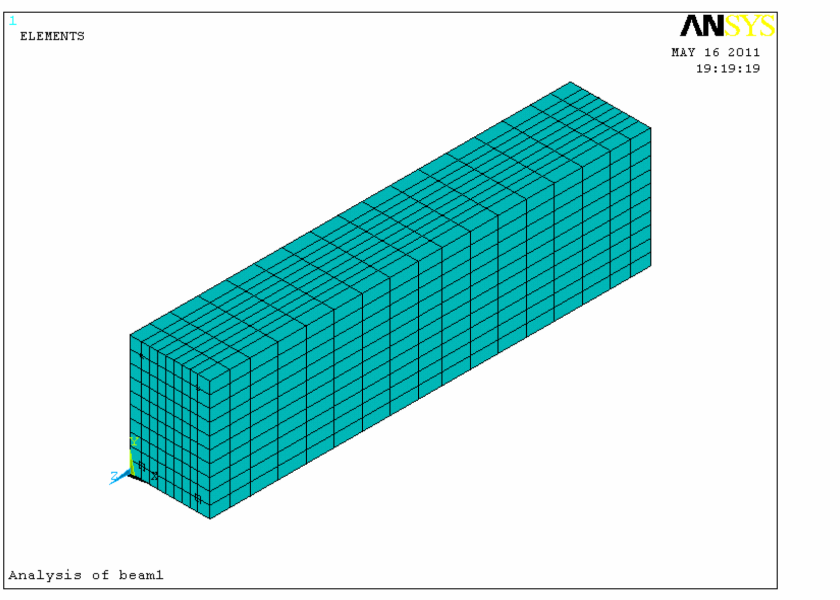

Figure 7: Concrete element model

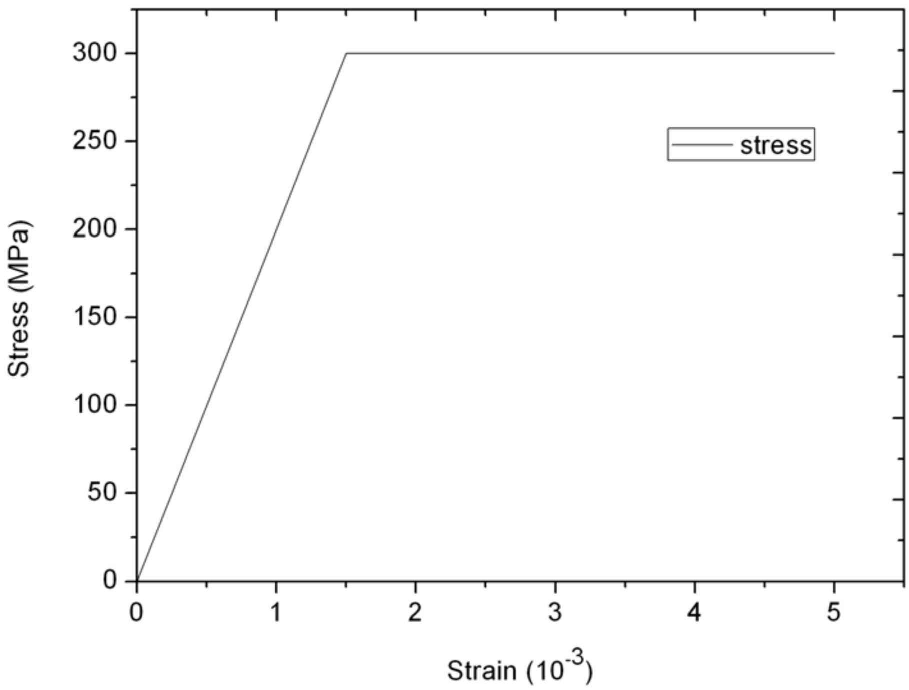

Figure 8: Bilinear isotropic hardening (BISO) model of the bar

Consolidated-Node Model

In this model, the Solid65 element was adopted as concrete element whose initial elastic modulus is 13585Mpa, Poisson ratio is 0.2. Its yield criterion is multilinear isotropic hardening (MISO) model, as shown in Fig.6. The uniaxial compressive strength is 14.3MPa, the uniaxial tensile strength is 1.43MPa, crack opening shear transfer coefficient is 0.5, crack closing shear transfer coefficient is 0.95. The concrete model is shown in Fig.7.

Elastic modulus of Link8 element (bar element) is 2×10^5 MPa and its Poisson ratio is 0.3. The yield strength of the bottom bars is 300MPa and the yield strength of the stirrups is 210MPa. BISO model (see Fig.8) is adopted for the bar element. The bar model is shown in Fig. 9.

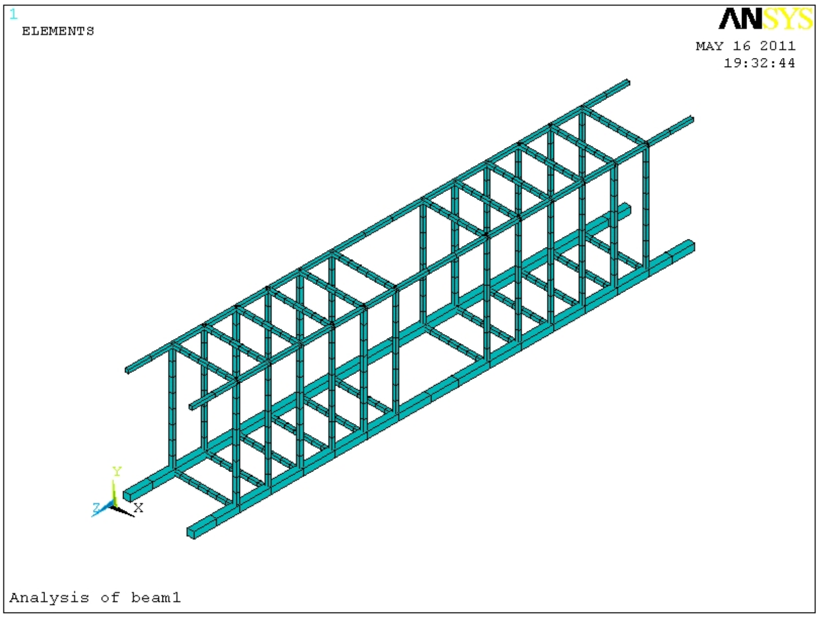

Figure 9: Bar element model

The nodes of bar element and the concrete element at the same location were consolidated. The displacement constraints (3-d and 2-d) were respectively applied on the concrete nodes at the bearing position on both sides. The concentrated load was applied in both sides of the mid-span and the distance from the mid-span is 50mm. The simply supported RC beam with load and bearings is shown in Fig.10. The nonlinear analysis on load carrying capacity of the model beam was carried out and the obtained load-deflection curve is drawn in Fig.11.

From Fig.11, it can be seen that the relationship between the load and deflection is linear when the force applied on the simply supported beam is small (with the load larger). As the load increased, the tensile crack in the concrete appeared and the load-deflection curve has changed, which shows that the increasing speed of the deflection becomes faster. At last, the tensile reinforcement yielded, plastic hinge appeared and the load-displacement curve became nearly horizontal. The ultimate load carrying capacity of the model is 42.5kN and the theoretical capacity is 43.0kN, which indicates that the consolidated-node model is correct.

FE Model with Combin39 Element

Based on the FE model in the first step, Combin39 element was installed between the bar element node of longitudinal bar and the concrete element node to consider the bonding slip at the bar-concrete interface. The nonlinear analysis of the FE model considering bond-slip was carried out and the new load-deflection curve was obtained as shown in Fig.12. Comparing the ultimate load carrying capacity of the model (43.1kN) with the theoretical capacity (43.0kN), it can be concluded that it is reasonable to use Combin39 element in FE model and the FE model with Combin39 element is feasible to analyze for the load carrying capacity of corroded RC beam.

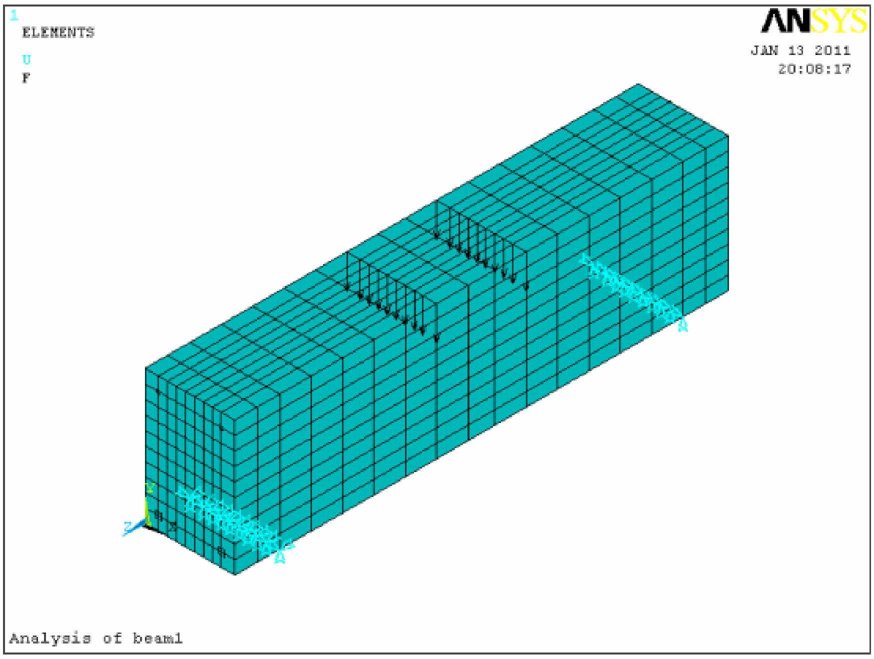

Figure 10: Consolidated supported beam model

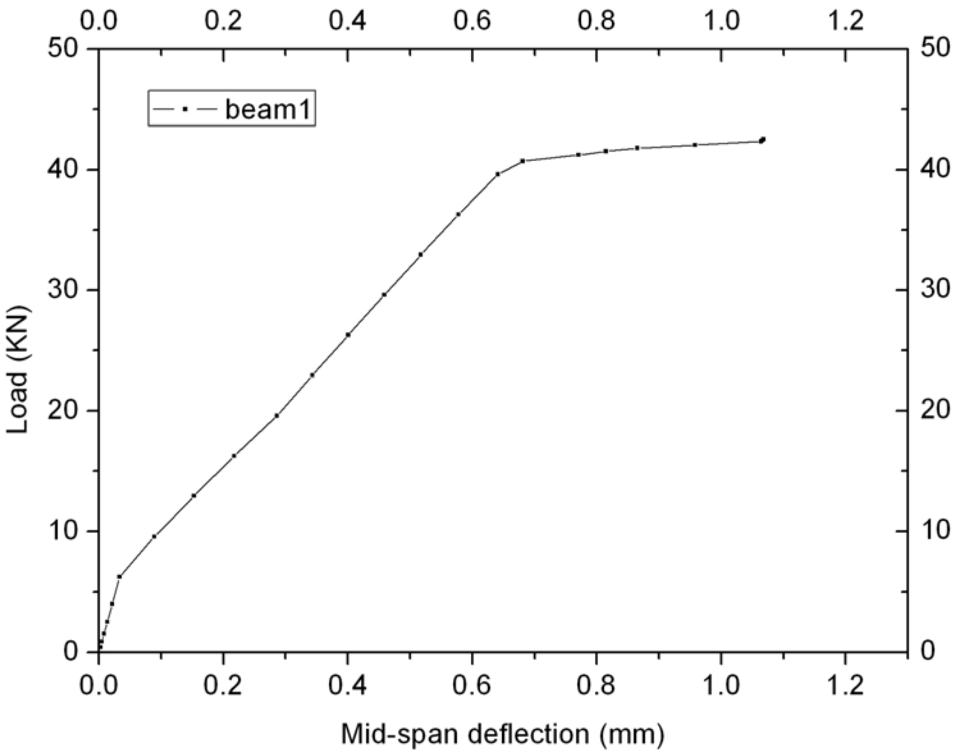

Figure 11: Load-deflection of the consolidated model

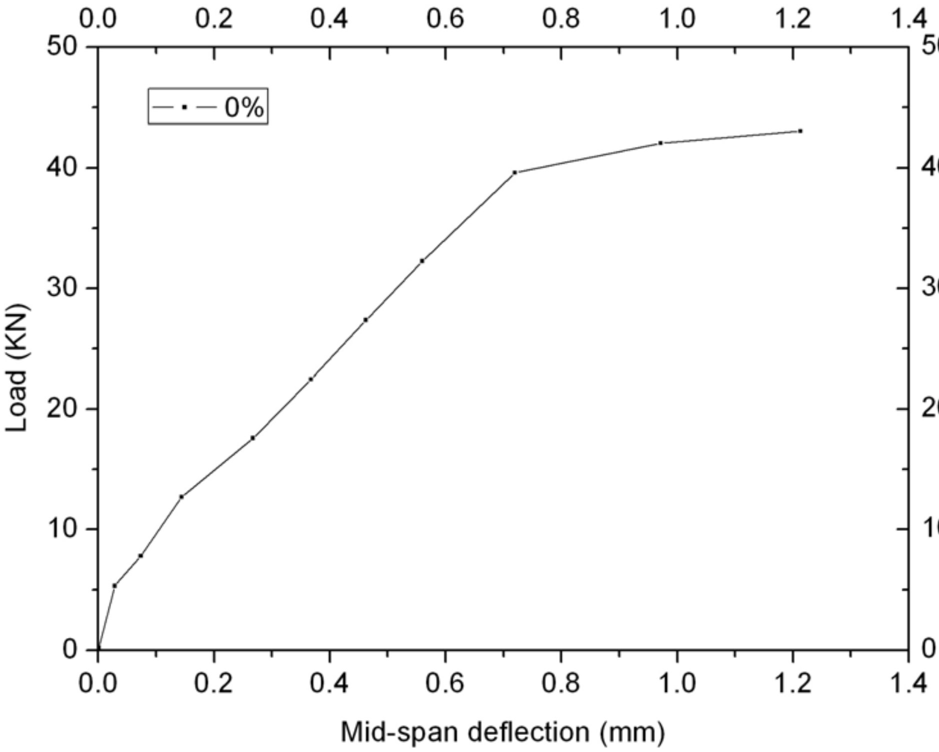

Figure 12: Load-displacement curve with the spring element

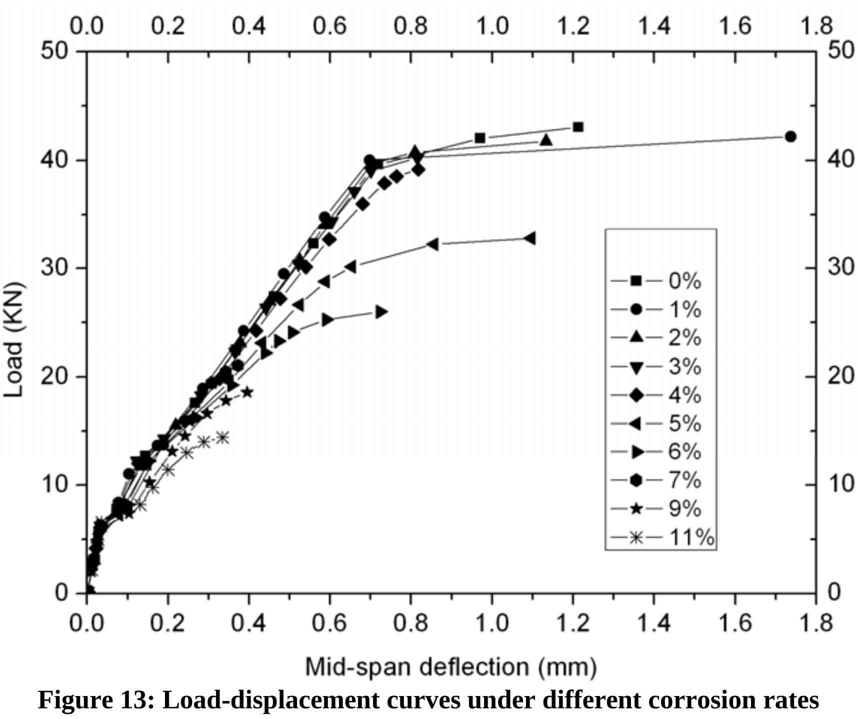

Figure 13: Load-displacement curves under different corrosion rates

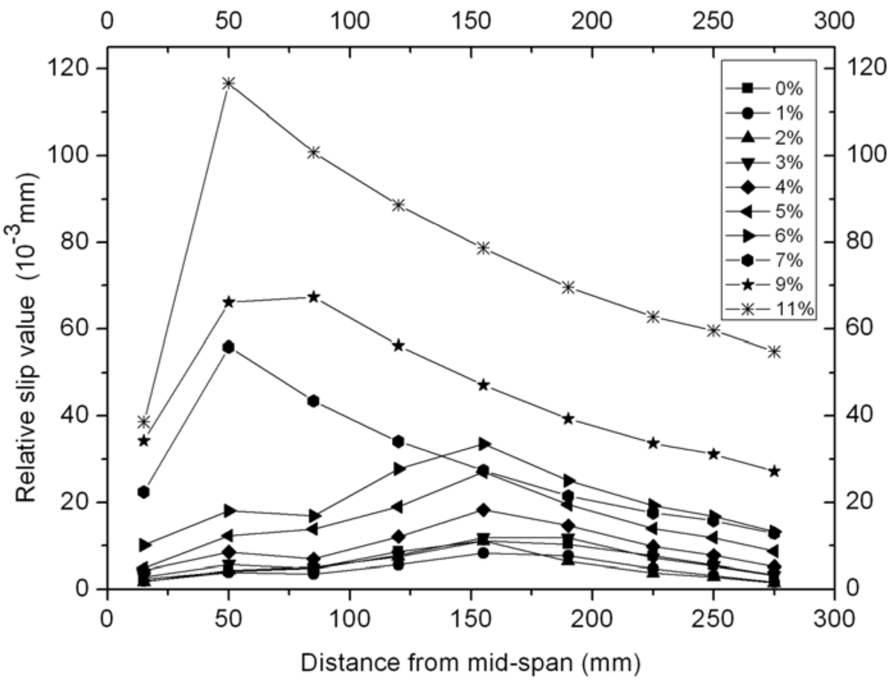

Figure 14: The effect of corrosion rate on the slip value at the bar-concrete interface

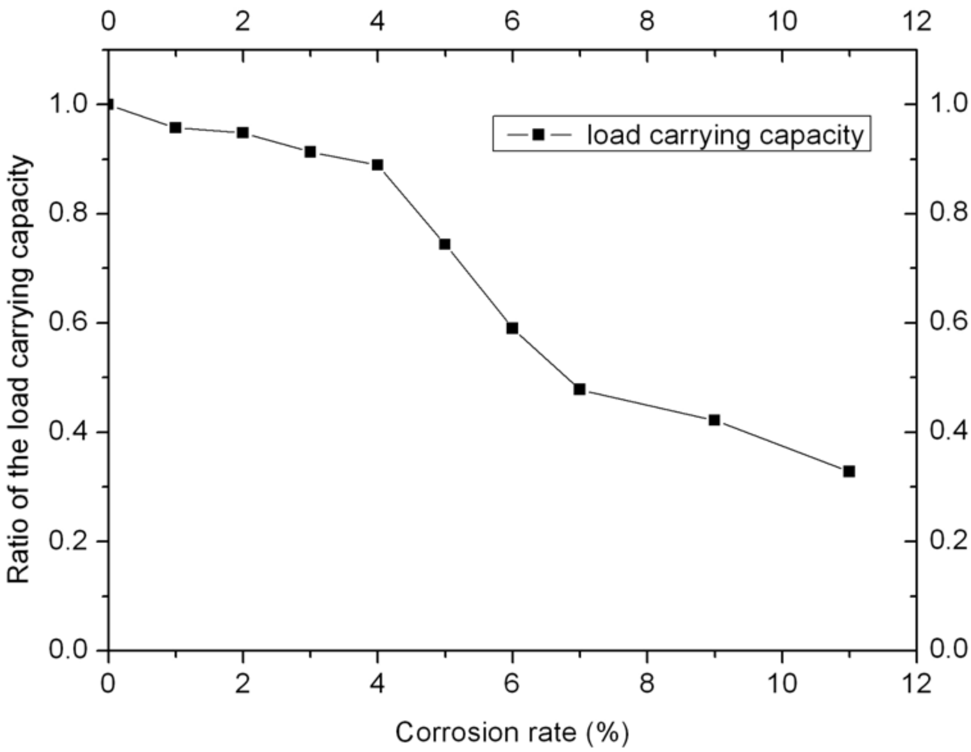

Figure 15: The effect of the corrosion on the load carrying capacity

Simulation of Steel Corrosion

Through modifying the parameters of Combin39 element, the different corrosion rates (1%, 2%, 3%, 4%, 5%, 6%, 7%, 9%, 11%) can be simulated. Then the models of corroded RC beams with different corrosion rates were built. The nonlinear analysis of these FE models on load carrying capacity was carried out and the new load-deflection curves are obtained as shown in Fig.13.

From Fig.13, it has been found that the relationship between the load and deflection is also linear and the change of deflection with the corrosion rate increase is not obvious when the force applied on the simply supported beam is small. With the increase of the applied force, the tensile crack in the concrete appears and load-deflection curves change and the increasing speed of the deflection becomes faster. Further, the larger the corrosion is, the faster is the increase of deflection. Besides, the failure mode is greatly affected by the corrosion rate; that is, when the corrosion rate is low, the failure mode of simply supported RC beam is ductile failure, however with the corrosion rate increasing, yield platform becomes shorter and the failure mode turns to brittle failure.

DISCUSSION

Effect of Corrosion Rate on Member Rigidity

Fig.13 shows that the corrosion rate has little effect on cracking load and rigidity of the simply supported beam before cracking, which indicates that the beam is in the stage of elastic condition. After the tensile crack in the concrete appears, the member rigidity declines a little. The decrease of rigidity has a close relationship with the corrosion rate. The larger the corrosion rate is, the larger is the decreasing extent of rigidity. At low corrosion rate, the tensile concrete crack does not immediately cause the large slip value at the bar-concrete interface, while with the growth of the corrosion rate the tensile concrete crack will cause the large slip value at the bar-concrete interface in a short moment, which leads to the larger decrease of rigidity. Besides, it can be found that the yield platform of the load-displacement curve becomes narrow with the corrosion rate increase, which means that the failure mode of simple supported RC beam is changed from the ductile failure to the brittle failure with the increase of the corrosion.

The Effect of Corrosion Rate on the Slip Value at the Bar-Concrete Interface

Under the same load and the different corrosion rates, the slip curve at the bar-concrete interface in the right half span of the simply supported beam along the longitudinal direction is shown in Fig.14. The tensile concrete crack appears at the location denoted by the curve peak in which the slip value is the largest. When the corrosion rate is from 1% to 6%, there is a similar curve peak at the distance of 150mm from the mid-span, which indicates that the tensile crack in concrete appears at the same location. When the corrosion rate is from 7% to 11%, the curve peak is at the distance of 50mm from the mid-span instead, which indicates that the crack moves to the mid-span. Besides, with the growth of the corrosion rate, the curve arises integrally, which indicates that the slip value at the bar-concrete interface evenly increases at every location along the longitudinal bar.

The Effect of Corrosion Rate on the Load Carrying Capacity

Fig. 15 shows the relationship between the corrosion rate and the ratio of load carrying capacity of non-corrosion RC beam to that of RC beam with different corrosion rates. When the corrosion rate is low, the reinforcement corrosion has a small effect on the load carrying capacity. When the corrosion rate grows, the effect of the corrosion rate on the load carrying capacity is gradually significant and the descending speed of the ratio is the fastest with the corrosion rate (4%-7%), and then the descending speed becomes slow after that.

CONCLUSIONS

From the results of numerical simulation on corroded RC beam, the following conclusions can be drawn:

(1) Numerical simulation is effective to analyze the load carrying capacity of corroded reinforced concrete components, and it can overcome the disadvantages and does not have the limitations of experimental conditions and testing technology.

(2) The growth of the corrosion rate has little effect on the cracking load and the beam rigidity before the cracking of the tensile concrete appears. After cracking, the beam rigidity had a decline; the larger the corrosion rate is, the larger is the decreasing extent of rigidity.

(3) Reinforcement corrosion causes gradual degradation of the bond behavior at the bar-concrete interface. The slip value at the bar-concrete interface becomes large due to corrosion, and the larger the corrosion rate is, the larger is the slip value.

(4) Reinforcement corrosion leads to the decline of load carrying capacity of the simply supported RC beam. When the corrosion rate is in the range of 4%-7%, the descending speed of load carrying capacity is the fastest. Also, with the increase of the corrosion rate, the failure mode of simple supported RC beam is changed from the ductile failure to the brittle failure.

Acknowledgements

The financial support from the National Natural Science Foundation of China under grant number 51008148 is greatly acknowledged.

REFERENCES

Alexandros, N.K. and Imran, R. M. 2010. Finite element investigation of the structural response of corroded RC beams. *Engineering Structures*, 32 (9): 2984-2994.

Bertoa, L., Simionib, P. and Saettab, A. 2008. Numerical modelling of bond behaviour in RC structures affected by reinforcement corrosion. *Engineering Structures*, 30 (5): 1375-1385.

Coronelli, D. and Gambarova, P. 2004. Structural assessment of corroded reinforced concrete beams: modeling guidelines. *Journal of Structural Engineering, ASCE*, 130 (8):1214-1224.

Haskett, M., Oehlers, D.J. and Mohamed Ali, M.S. 2008. Local and global bond characteristics of steel reinforcing bars. *Engineering Structures*, 30 (2): 376-383.

Malumbela, G., Alexander, M. and Moyo, P. 2010. Variation of steel loss and its effect on the ultimate flexural capacity of RC beams corroded and repaired under load. *Construction and Building Materials*, 24 (6): 1051-1059.

Sharifi, Y. and Pai, J.K. 2011. Ultimate strength reliability analysis of corroded steel-box girder bridges. *Thin-Walled Structures*, 49 (1): 157-166.

Shi, Jinjie and Sun, Wei. 2010. Recent research on steel corrosion in concrete. *Journal of the Chinese Ceramic*, 38 (9):94-99.

Shodj, H. M., Kiani, K. and Hashemian, A. 2010. A model for the evolution of concrete deterioration due to reinforcement corrosion. *Mathematical and Computer Modelling*, 52 (9-10): 1403-1422.

Tapan, M. and Aboutaha, R.S. 2011. Effect of steel corrosion and loss of concrete cover on strength of deteriorated RC columns. *Construction and Building Materials*, 25 (4): 2596-2603.

Wang, Xiao-Hui, Gao, Xiang-Hua, Li, Bing and Deng, Bao-Ru. 2011. Effect of bond and corrosion within partial length on shear behaviour and load capacity of RC beam. *Construction and Building Materials*, 25 (4): 1812-1823.

Weiliang, J., Jin, X., Aoyu, J. and Hailong, W. 2009. Flexural capacity of corrosion-damaged RC beams. *China Civil Engineering Journal*, 42 (11): 64-70.

Xu, S. 2003. The models of deterioration and durability evaluation of reinforced concrete structure[D]. XI'an University of Architecture and Technology.

Yuan, Yingshu and Ji, Yongsheng. 2009. Modeling corroded section configuration of steel bar in concrete structures. *Construction and Building Materials*, 23 (6): 2461-2466.